LBNL-48976
Preprint

ERNEST ORLANDO LAWRENCE BERKELEY NATIONAL LABORATORY

Fast Phase Space Computation of Multiple Arrivals

S. Fomel and J.A. Sethian

Computing Sciences Directorate
Mathematics Department

September 2001

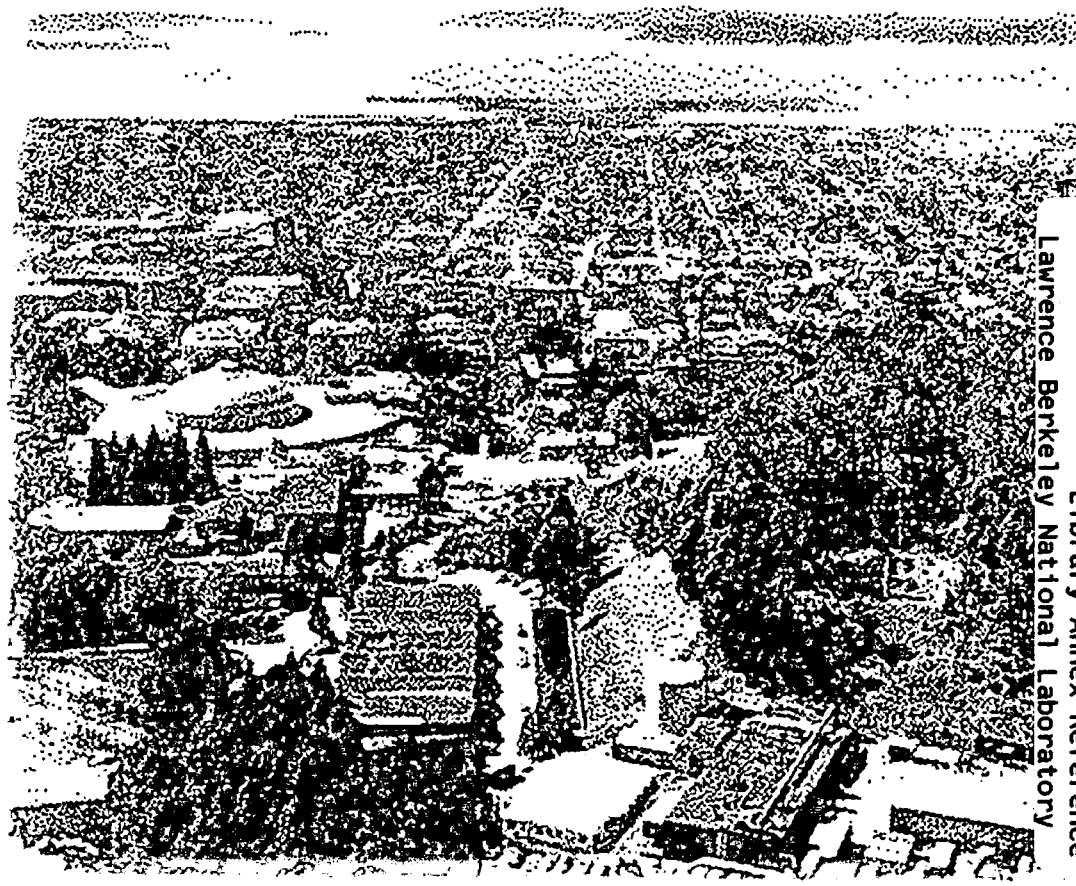

REFERENCE COPY
Does Not
Circulate
Library Annex Reference
Lawrence Berkeley National Laboratory
LBNL-48976
Copy 1

DISCLAIMER

This document was prepared as an account of work sponsored by the United States Government. While this document is believed to contain correct information, neither the United States Government nor any agency thereof, nor the Regents of the University of California, nor any of their employees, makes any warranty, express or implied, or assumes any legal responsibility for the accuracy, completeness, or usefulness of any information, apparatus, product, or process disclosed, or represents that its use would not infringe privately owned rights. Reference herein to any specific commercial product, process, or service by its trade name, trademark, manufacturer, or otherwise, does not necessarily constitute or imply its endorsement, recommendation, or favoring by the United States Government or any agency thereof, or the Regents of the University of California. The views and opinions of authors expressed herein do not necessarily state or reflect those of the United States Government or any agency thereof or the Regents of the University of California.

LBNL-48976

Fast Phase Space Computation of Multiple Arrivals

S. Fomel and J.A. Sethian

Computing Sciences Directorate
Mathematics Department
Ernest Orlando Lawrence Berkeley National Laboratory
University of California
Berkeley, California 94720

September 2001

This work was supported by the Director, Office of Science, Office of Advanced Scientific Computing Research, Mathematical, Information, and Computational Sciences Division, of the U.S. Department of Energy under Contract No. DE-AC03-76SF00098.

Fast Phase Space Computation of Multiple Arrivals

S. Fomel and J.A. Sethian *

Dept. of Mathematics
University of California, Berkeley 94720

Submitted For Publication,
Proceedings of the National Academy of Sciences, Sept. 9, 2001

Sept. 7, 2001

Abstract

We present a fast, general computational technique for computing the phase-space solution of static Hamilton-Jacobi equations. Starting with the Liouville formulation of the characteristic equations, we derive "Escape Equations" which are static, time-independent Eulerian PDEs. They represent all arrivals to the given boundary from all possible starting configurations. The solution may be parameterized as a family of hypersurfaces; which we numerically produce through a 'one-pass' formulation, building on ideas from semi-Lagragian methods and Fast Marching Methods. The resulting technique is of computational order $O(N \log N)$, where N is the total number of points in the computational domain. Unlike a ray-tracing approach, which starts with a given source (or sources) on the boundary, and recomputes the entire solution each time these sources are changed, in this formulation the same result is achieved in postprocessing once the essential solution has been obtained. As an application, we apply the technique to the problem of computing first, multiple, and most energetic arrivals to the Eikonal equation.

1 Introduction

We present a fast, general computational technique for computing phase space solutions of static Hamilton-Jacobi equations. We derive a set of "Escape equations" which are static, time-independent Eulerian partial differential equations which represent all arrivals to the given boundary from all possible starting configurations. The solution of the Escape Equations may be parameterized as a family of hypersurfaces. We follow the strategy proposed in [14] and solve these Escape Equations by systematically constructing these hypersurfaces in increasing order, using a 'one-pass' formulation. This means that the solution at each point in the computational mesh is computed only k times, where k does not depend on the number of points in the mesh. The algorithm combines ideas of semi-Lagrangian methods and Fast Marching Methods [27]. Unlike a ray-tracing approach, which starts with a given source (or sources) on the boundary, and recomputes the entire solution each time these sources are changed, in this formulation the same result is achieved in postprocessing once the essential solution has been obtained. We demonstrate the applicability of this technique by computing multiple arrivals to the Eikonal equation in a variety of settings.

*This work was supported in part by the Applied Mathematical Sciences subprogram of the Office of Energy Research, U.S. Department of Energy, under Contract Number DE-AC03-76SF00098, and the Office of Naval Research under under grant FDN00014-96-1-0381.

2 Formulation of Problem

Consider the static Hamilton-Jacobi equation
$H(x, \nabla u) = 0$. A nonlinear Hamiltonian H may not have a unique solution, even with smooth boundary data and smooth H. A particular, *viscosity-type* solution can be selected [8, 9], corresponding to the earliest arrival from the given boundary. Fast algorithms for computing these viscosity-satisfying first arrival solutions have been developed in recent years, in particular, the Fast Marching Method, developed by Sethian [27] for computing the solution to the Eikonal equation [27] and "Ordered Upwind Methods (OUM)", introduced by Sethian and Vladimirksy [30, 31] for computing the solution of convex static Hamilton-Jacobi equations which arise in anisotropic front propagation and optimal control. These first arrivals are of considerable importance in a large collection of problems such as computing seismic travel times [28]; see [29, 34] for reviews.

However, later arrivals may carry additional valuable information, and it is often desirable to compute all possible solutions. For example, in geophysical simulations, first arrivals may not correspond to the most energetic arrivals, and this can cause problems in seismic imaging [1, 16].

There are two approaches to computing these multiple arrivals.

- The Lagrangian (ray tracing) approach [5, 25] and its variations [26, 36]. Here, the phase space characteristic equations are integrated, often from a source point, resulting in a Lagrangian structure which fans out over the domain. This is a valuable and common approach, however it can face difficulties either in low ray density zones where there are very few rays or near caustics where rays cross; in addition, the use of irregular computational grid is often inconvenient.

- Rather than work in phase space, the second approach is to work with the static Hamilton-Jacobi equation itself, and attempt to extract multiple arrivals. In recent years, this has led to many fascinating and clever Eulerian PDE-based approaches to computing multiple arrivals, including slowness matching algorithms [33], dynamic surface extension algorithms [32] and its modification [24], segment projection methods [12], and "big-ray tracing" [2]; see also [3].

The approach presented in this paper computes the solution in phase space, but does so in a reduced Eulerian partial differential equations framework. Thus, we compute **all the arrivals from all points.** In applications such as tomography and seismic migration, one needs to solve multiple boundary problems with $H(x, \nabla u) = 0$ and the point-source boundary condition $u(x) = 0$ for $x = s$ with multiple sources s distributed on the surface of the observational domain. In this case, the solutions span $(2n-1)$-dimensional space, composed of x and s. The computational advantage of our approach is that by transforming the problem to a reduced Eulerian setting, we develop a linear, time-independent equation boundary value problem in $(2n-1)$ phase space, whose solution may be constructed using a very fast ordering scheme. One can use the output of such computation either for extracting multiple arrivals for a particular set of sources or directly, as in the method of angle-gather migration [35].

The regularity of the phase space has been utilized previously in theoretical studies on the asymptotic wave propagation [23, 11]. In this paper, we utilize it for developing an efficient computational technique.

3 Formulation of Equations

3.1 Lagrangian Formulation of Phase-Space Solution

We begin with the static Hamilton-Jacobi equation:

$$H(x, \nabla u) = 0. \tag{1}$$

and write the well-known characteristic equations in phase space (x, p), where p corresponds to ∇u (see, for example, [13]). Let σ is a parameter varying along the trajectory. Differentiating Eqn. 1 with respect to σ, we obtain

$$\nabla_x H \cdot \frac{dx}{d\sigma} + \nabla_p H \cdot \frac{dp}{d\sigma} = 0, \tag{2}$$

where the Hamiltonian H is assumed to be twice continuously differentiable. This equation is satisfied when the characteristics obey

$$\frac{dx}{d\sigma} = \nabla_p H; \qquad \frac{dp}{d\sigma} = -\nabla_x H \tag{3}$$

Differentiating the function $u(x(\sigma))$, we obtain an additional equation for transporting the function u along the characteristics:

$$\frac{du}{d\sigma} = \nabla u \cdot \frac{dx}{d\sigma} = p \cdot \nabla_p H \tag{4}$$

The system given by Eqns. 3,4 can be initialized at $\sigma = 0$: $x(0) = x_0$, $p(0) = p_0$, $u(0) = 0$.

In the Lagrangian approach, one computes the solution of the point-source Hamilton problem by starting at a source point x_0, scanning through different initial values of p_0 and filling the x space with trajectories that follow Eqns. 3. The strength of this approach is in the fact that the solution is uniquely defined in the phase space by following individual trajectories. However, when the trajectories collide, the solution in the physical space becomes multi-valued and interpolating it onto a regular x grid presents a difficult computational problem [21].

3.2 Liouville Formulation of Phase-Space Solution

We now convert this into a set of Liouville equations; these have been used extensively by Chorin, Hald, and Kuperfman [6, 7]. Eqns. 3,4 form a system of coupled ordinary differential equations, starting with a particular set of initial conditions. The Liouville equation is a partial differential equation for the same solution with the differentiation performed with respect to the initial conditions; it describes the local change in the solution in response to changes in the initial conditions.

To simplify notation, let denote the phase-space vector (x, p), by y, the right-hand side of system given in Eqn. 3 by vector function $R(y)$, and the right-hand side of Eqn. 4 by the function $r(y)$. In this notation, the Hamilton-Jacobi system takes the form

$$\frac{\partial y(y_0, \sigma)}{\partial \sigma} = R(y); \qquad \frac{\partial u(y_0, \sigma)}{\partial \sigma} = r(y), \tag{5}$$

and is initialized at $\sigma = 0$ as $y = y_0$ and $u = 0$.[1]

In the Appendix, we show that the solution of system (5) as a function of both the trajectory parameter σ and the initial condition y_0 satisfies the Liouville partial differential equations

$$\frac{\partial y(y_0, \sigma)}{\partial \sigma} = \nabla_0 y \, R(y_0) \ , \tag{6}$$

and the transported function u satisfies the analogous equation

$$\frac{\partial u(y_0, \sigma)}{\partial \sigma} = \nabla_0 u \, R(y_0) + r(y_0) \ , \tag{7}$$

where ∇_0 denotes the gradient with respect to y_0. These are the Liouville equations.

3.3 Formulation of the Stationary "Escape" Equations

Assume that there exists a closed boundary $\partial\mathcal{D}$ in the y space that is crossed by every characteristic trajectory that originates in $y_0 \in \mathcal{D}$. This defines for every y_0 the function $\sigma = \widehat{\sigma}(y_0)$ of the first crossing of the corresponding characteristic with $\partial\mathcal{D}$.

Let us now introduce a differentiable function $\Gamma(y)$ that identifies the boundary, that is, $\Gamma(y) = 0$. In particular, we then have that $\Gamma\left(y(y_0, \widehat{\sigma}(y_0)\right) = 0$. We can differentiate with respect to the initial condition y_0 to obtain

$$\Gamma'(y) \left[\nabla_0 y + \frac{\partial y}{\partial \sigma} \nabla_0 \widehat{\sigma}\right] = 0 \ . \tag{8}$$

[1] The full y space has $2n$ variables. However, by using the Hamilton equation $H(y) = 0$ as an additional constraint, we can often reduce the Hamilton-Jacobi system (5) to $2n - 1$ equations of the same form. Therefore, we can assume that y has $2n - 1$ independent components.

Multiplying equation (8) by $R(y_0)$ and using the Liouville equation (6), we obtain

$$\Gamma'(y)\,\frac{\partial y}{\partial \sigma}\,[1+\nabla_0\widehat{\sigma}\cdot R(y_0)]=0\,. \tag{9}$$

Eqn. 9 will be satisfied if the function $\widehat{\sigma}(y_0)$ satisfies the differential equation

$$1+\nabla_0\widehat{\sigma}\cdot R(y_0)=0\,. \tag{10}$$

We can also define the escape location $\widehat{y}(y_0)=y\,(y_0,\widehat{\sigma}(y_0))$. Differentiating with respect to y_0 yields

$$\nabla_0\widehat{y}=\nabla_0 y+\frac{\partial y}{\partial \sigma}\,\nabla_0\widehat{\sigma}\,. \tag{11}$$

Multiplying both sides of equation (11) by $R(y_0)$ and applying equations (6) and (10) leads to the homogeneous differential equation

$$\nabla_0\widehat{y}\,R(y_0)=\nabla_0 y\,R(y_0)+\frac{\partial y}{\partial \sigma}\,\nabla_0\widehat{\sigma}\cdot\,R(y_0)=0\,. \tag{12}$$

Using a similar argument and equations (7) and (10) the escape value $\widehat{u}(y_0)=u\,(y_0,\widehat{\sigma}(y_0))$ can be shown to satisfy the equation

$$\nabla_0\widehat{u}\cdot R(y_0)+r(y_0)=0\,. \tag{13}$$

Eqns. 12-13 have the following boundary conditions: $\widehat{y}(y_0)=y_0$ and $\widehat{u}(y_0)=0$ if y_0 lies on $\partial\mathcal{D}$, and the corresponding characteristic flows out of $\mathcal{D}$.

These are the static "escape" equations (12-13) that we will numerically approximate to solve the multiple arrival problem. We note that the functions $\widehat{u}(y_0)$, $\widehat{y}(y_0)$, and $\widehat{\sigma}(y_0)$ provide values for u, y, and σ respectively obtained at the boundary for a trajectory starting at the point in phase space y_0. The equations that describe these functions are linear and possess unique solutions.

Escape Equations

$$\begin{aligned}1+\nabla_0\widehat{\sigma}\cdot R(y_0)&=0\\ \nabla_0\widehat{y}\,R(y_0)&=0\\ \nabla_0\widehat{u}\cdot R(y_0)+r(y_0)&=0\end{aligned} \tag{14}$$

To summarize, rather than compute in physical space x, we have transformed the problem to phase-space $y=(x,p)$. However, there are two distinct differences between our approach and the typical characteristic ray-tracing approach to computing in phase space:

- First, we have transformed the problem into a linear partial differential equations with the differentiation with respect to the initial conditions. In the next section, we present a fast technique for computing the solution to these equations.
- Second, and equally importantly, the solution to these equations can be constructed without regards to any particular boundary conditions and/or placement of sources. Unlike a ray-tracing approach, which starts with a given source (or sources) on the boundary, and must recompute the entire solution each time these sources are changed, in this formulation this may be done in postprocessing once the essential solution has been obtained. As an example, once the $\{\widehat{u}(y_0),\widehat{y}(y_0),\widehat{\sigma}(y_0)\}$ field has been computed, we are then free to extract first arrivals, later arrivals, arrivals at a particular source on the boundary, etc.

3.4 Example: The Eikonal equation

As an example, which will serve as our computational test, the Hamiltonian for the Eikonal equation can be written in the form

$$H(x,p) = \frac{1}{2}p \cdot p - \frac{1}{2}n^2(x) = 0 \,, \tag{15}$$

where $n(x)$ corresponds to the wave slowness (refraction index). In accordance with equations 3, the functions $R(y)$ and $r(y)$ are specified in this case to be

$$R(y) = \begin{pmatrix} \nabla_p H \\ -\nabla_x H \end{pmatrix} = \begin{pmatrix} p \\ n(x)\nabla n \end{pmatrix} \tag{16}$$

$$r(y) = p \cdot \nabla_p H = p \cdot p = n^2(x) \,. \tag{17}$$

Correspondingly, the escape equations transform to

$$\nabla_{x_0}\widehat{y}\, p_0 + n(x_0)\, \nabla_{p_0}\widehat{y}\, \nabla_{x_0} n = 0 \tag{18}$$

$$\nabla_{x_0}\widehat{u} \cdot p_0 + n(x_0)\, \nabla_{p_0}\widehat{u} \cdot \nabla_{x_0} n + n^2(x_0) = 0. \tag{19}$$

3.4.1 Constant slowness

In the case when the refraction index n does not depend on the position, the escape equations take a simpler form

$$\nabla_{x_0}\widehat{y}\, p_0 = 0; \qquad \nabla_{x_0}\widehat{u} \cdot p_0 + n^2 = 0. \tag{20}$$

For a more specific example, let us consider the case of the region $\mathcal{D}$ defined by $z > 0$ and $p_z < 0$, where z is the first component of x_0, and p_z is the first component of p_0. The escape surface $z = 0$ corresponds to the Earth surface in Geophysics, while the condition $p_z < 0$ selects the up-going waves. Eqn. 20 is then supplied with the boundary conditions

$$\widehat{y}\,|_{z=0} = y_0; \qquad \widehat{u}\,|_{z=0} = 0. \tag{21}$$

The analytical solution of the problem 20-21 then takes the form $\widehat{z} = 0$, $\widehat{x}_i = x_i - \frac{p_i}{p_z} z$, $\widehat{p} = p_0$, and $\widehat{u} = -\frac{n^2 z}{p_z}$, where x_i is the ith component of x_0 with $i > 1$, and p_i is the corresponding component of p_0.

3.4.2 One-dimensional slowness

Another specific example of the eikonal equation is the case of a one-dimensional slowness function. If the boundary conditions take the form of Eqn.21, while the slowness $n(x)$ only depends on the first component of x, then Eqn. 19 simplifies to

$$\frac{\partial \widehat{u}}{\partial z} p_z + n'(z)\, n(z)\, \frac{\partial \widehat{u}}{\partial p_z} + n^2(z) = 0 \,. \tag{22}$$

Letting $p_h = \sqrt{n^2(z) - p_z^2}$, Eqn. 22 becomes

$$-\frac{\partial \widehat{u}}{\partial z}\sqrt{n^2(z) - p_h^2} + n^2(z) = 0 \tag{23}$$

whose analytical solution is

$$\widehat{u} = \int_0^z \frac{n^2(\xi)\, d\xi}{\sqrt{n^2(\xi) - p_h^2}} \,. \tag{24}$$

Using similar transformations, the escape equations (18) resolve to $\widehat{z} = 0$, $\widehat{x}_i = x_i + \int_0^z \frac{p_i\, d\xi}{\sqrt{n^2(\xi) - p_h^2}}$, $\widehat{p}_z = -\sqrt{n^2(0) - p_h^2}$, and $\widehat{p}_i = p_i$.

There formulas are well-known in the theory of Lagrangian ray tracing in one-dimensional media [5]. We obtained them here as the solution of the escape PDEs for the Eulerian formulation of the same problem.

3.4.3 Amplitude computation

A common use of the eikonal equation is for describing the wave propagation in the high-frequency asymptotics [5]. Here, the eikonal equation is often supplemented with the amplitude transport equation for computing not only the wavefront position but also the corresponding wave amplitude.

In the high-frequency asymptotics, the leading order amplitude contribution comes from the geometrical spreading: a measure of the ray tube focusing effect. We can extract the geometrical spreading information directly from the phase-space solution of the escape PDEs. Indeed, according to the known formula [17, 18], the squared amplitude is inversely proportional to

$$A^{-2} \sim |\det [\nabla_{p_i} \widehat{x}_i] \, p_z \, \widehat{p}_z| \ , \tag{25}$$

where p_z and $\widehat{p}_z$ are the components of p_0 and $\widehat{p}$, normal to the observational boundary, and p_i and $\widehat{x}_i$ correspond to the remaining components.

In the case of multiple arrivals, we can use the simple access to the amplitude information, provided by formula (25) to select the most energetic arrival from all the branches of the solution.

4 Numerical Algorithm

The numerical algorithm proposed in [14] is to solve Eqns. 18,19 for a numerical computations of traveltimes on a fixed x, z grid.[2] Although both $\widehat{u}(y_0)$ and $\widehat{y}(y_0)$ are strictly single-valued, we later can extract from them the possibly multi-valued traveltimes from every grid point x, z to a point on the boundary.

4.1 The Geometry of the Solution

We illustrate the geometry behind the algorithm through an instructive example. Consider a square, and suppose we wish to find the time $\widehat{u}(x, z, \theta)$ at which a ray leaving the initial point (x, z) inside the square, initially moving in direction θ, hits the boundary. We assume that the slowness field $n(x, z)$ is given. First, note that the level surface $\widehat{u}(x, z, \theta) = T$, drawn in x, z, θ space, gives the set of all initial positions and directions which reach the boundary of the square at time T. By the uniqueness of characteristics, the family of hypersurfaces parameterized by T and given by

$$\widehat{U}(T) = \{x, z, \theta \ \mid \ \widehat{u}(x, z, \theta) = T\} \tag{26}$$

sweep out the solution space. In Figure 1a, we show the level surface $\widehat{u}(x, z, \theta) = .3$ for the collapsing square.

Eqn. 19 is a linear equation for the arrival field $\widehat{u}$ and thus we know the characteristic direction at every point of the phase space x, p. We introduce an algorithm designed in the spirit of Fast Marching Methods [27]; we march the solution surface outwards from the boundary, using the characteristic direction to update grid values. We note that the ordering is considerably easier to achieve than the one for optimal control developed in [30], since there the characteristic direction is not known.

Our algorithm is quite similar to ordering process for transport equations which have a considerably history, see [22] for an early work and [19] for a recent parallel implementation. We refer the reader to a large collection of early work on characteristic methods for ordering update sequences for linear transport problems.

4.2 Algorithm

Consider a discretization of phase space; in two space dimensions, this can be written as $\widehat{u}_{ijk}$, where the indices i, j, k run over x, z, and p respectively. Following the terminology of Fast Marching Methods [27] and Ordered Upwind Methods [30, 31], the nodes are divided into three classes: *Far* (no information about the correct value of $\widehat{u}_{ijk}$ is known), *Accepted* (the correct value of $\widehat{u}_{ijk}$ has been computed), and *Considered* (adjacent to *Accepted*), for which $\widehat{u}_{ijk}$ has already been computed, but may be corrected by a later computation.

[2] For ease of explanation in this section, we switch to the notation in which a physical domain is given by x, z, and we let θ be the angle between the vertical and the vector p.

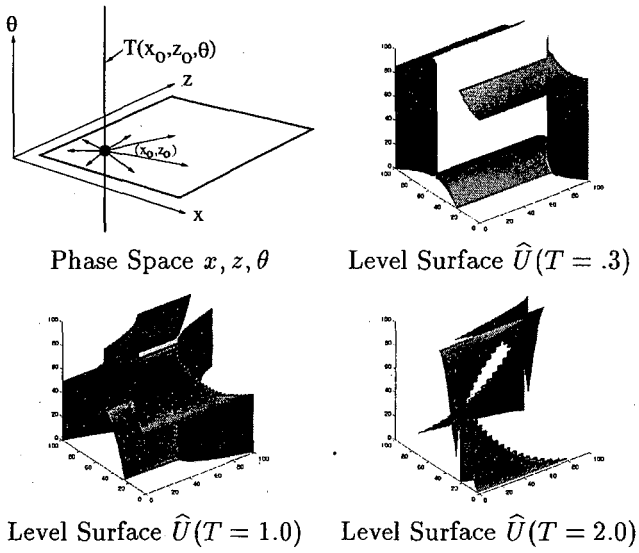

Figure 1: Geometry of Solution Surface

We note that standing at any grid point, we can compute the value $\widehat{u}_{ijk}$ using a discrete cell characteristic method, which traces back along the characteristic to the initial boundary (see, for example, [4, 20].) If we were to use this algorithm to compute $\widehat{u}_{ijk}$ at each grid point, we would have a cell-based Lagrangian ray-trace method. Instead, we use this technique to build the hypersurfaces in an outwards fashion.

Start with all nodes in *Far*. Put the boundary nodes in *Accepted*, and put all nodes adjacent to *Accepted* in *Considered*. Each *Considered* node is given a value by using a discrete cell characteristic method. If the characteristic at that node does not point back to the boundary, we assign it a large value. Then the algorithm is as follows (see Figure 2).

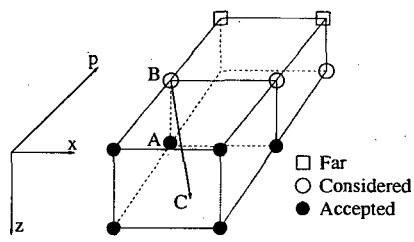

Figure 2: Point A has just been *Accepted*: *Considered* point B is updated by tracing characteristic back to point C and interpolating from *Accepted* values.

Algorithm

1. Take the *Considered* node with the smallest value for $\widehat{u}_{ijk}$ and make it accepted.
2. Find the octant that the characteristic direction going through that grid point points toward
3. For each neighboring grid point in that octant which is not *Accepted*, use the discrete cell characteristic update to compute a (possibly new) value for $\widehat{u}_{ijk}$ as follows (and, convert any such point which is *Far* to *Considered*): Trace backwards along the characteristic to intersect a cell face:
   (a) If all four values of that cell face are *Accepted*, use the interpolated value of $\widehat{u}_{ijk}$ at the intersection point, plus the update of $\widehat{u}_{ijk}$ along the drawn characteristic to produce the tentative value at ijk.

(b) If no points on that cell face are *Accepted*, do not update the value

(c) If more than one value of that cell face is *Accepted*, continue tracing along the characteristic by returning to (a).

4. Loop to (1) until all points are *Accepted*.

For higher accuracy, more than four points are used if available as accepted. Further details about the algorithm may be found in [15].

5 Results

5.1 Computation of Escape Solution

We begin in Figure 3 with a calculation of the full phase-space arrival field in a rectangular region. The slowness field corresponds to a Gaussian distribution around the center with peak slower than the surroundings (see Figure 5). On the upper left, we show the arrival position $\widehat{x}$ along the top wall ($z = 0$) of arrivals starting at a fixed slice $z = 0.9$ through the phase-space x, z, p cube. The vertical axis is the starting value p_o (actually, $\sin\theta$), and the horizontal axis is the starting value x_o; the color scale (shown in the bar on the right) is the arrival position $\widehat{x}$. On the upper right, we show the value of the arrival time $\widehat{u}$.

On the lower left, again limited to a fixed z slice, we show the x (horizontal axis) and p positions (vertical axis) of all trajectories that exit at the point $\widehat{x} = .5, z = 0$. Finally, in the figure on the lower right, again for a fixed z slice, we show the travel times $\widehat{u}$ required to reach the source exit point $\widehat{x} = .5, z = 0$, plotted against the *physical* space x (horizontal axis). Here, one sees the multiple arrival structure as expected, bending around the central slowness field and crossing over itself.

We emphasize that computing the solutions to the escape equations for different placement of sources as well as extracting multiple arrivals are all done as postprocessing of the computed solution.

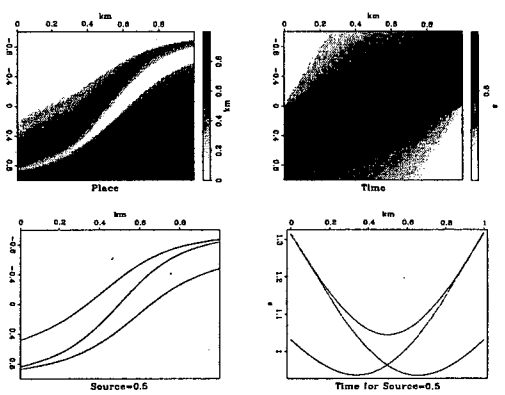

Figure 3: Computation of Escape Solutions

5.2 Extracting Multiple Arrivals

As a different and perhaps more geometrically familiar example, in Figure 4 we show the equiarrivals curves, which are the set of all points in physical space whose trajectories reach the boundary normal to the source distribution at the same time. In this case, the source distribution is the boundary of the entire square, thus we produce non-viscosity multiply-sheeted solution of a square propagating inward with unit speed. Again, we stress that the calculation need not be repeated to obtain equiarrivals from a different set of sources.

These multiple arrivals are extracted as follows: the front emanating from the boundary passes through the point x_o, z_o at time $\widehat{u} = T_{crit}$ if T_{crit} is a critical point of $T(x_o, z_o, p)$, where differentiation is taken with respect to p.

Thus, we merely locate the critical points of $\widehat{u}$ with respect to the variable p to determine the arrival front in the domain space.

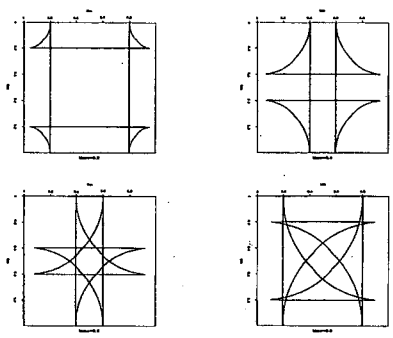

Figure 4: Multiple Arrivals from Square

5.3 Extracting Most Energetic Arrivals

As the last example, we show how to compute the most energetic arrival of the Eikonal equation from among all the potential arrivals using the amplitude computation discussed earlier. First, in Figure 5, the left pair shows all the arrivals starting from a source at the center of the top wall, together with the slowness field on the right (darker is slower). The right pair shows the first arrival and on the amplitude of the displayed arrival (the lighter the tone, the more amplitude).

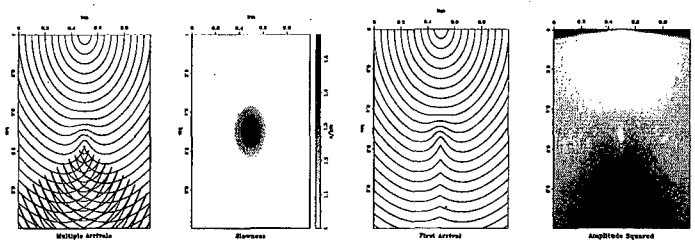

All arrivals First arrival

Figure 5: All vs. First arrivals

In contrast, in Figure 6 we show the most energetic arrival and the corresponding amplitude field.

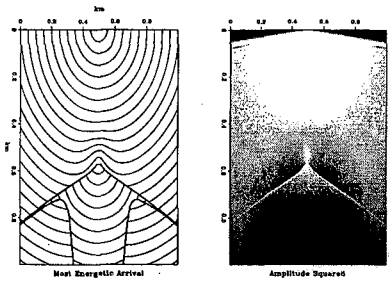

Figure 6: Most Energetic Arrival

More details about the numerical algorithms and further calculations may be found in [15].

6 Appendix: Liouville PDE

We wish to derive Eqns. 6, 7 [3]. First, we will consider the function

$$F(y_0, \sigma) = \frac{\partial y}{\partial \sigma} - \nabla_0 y\, R(y_0) = R(y) - \nabla_0 y\, R(y_0) \tag{27}$$

and prove that it is identically zero.

We note that at $\sigma = 0$, $y = y_0$ (the initial condition), $\nabla_0 y = 1$, and therefore $F(y_0, 0) = 0$. Next, differentiating F with respect to σ, we obtain

$$\begin{aligned} \frac{\partial F}{\partial \sigma} &= R'(y)\,\frac{\partial y}{\partial \sigma} - \nabla_0 \frac{\partial y}{\partial \sigma}\, R(y_0) \\ &= R'(y)\, R(y) - \nabla_0 R(y)\, R(y_0) \\ &= R'(y)\, [R(y) - \nabla_0 y\, R(y_0)] \\ &= R'(y) F(y_0, \sigma) \end{aligned} \tag{28}$$

As a function that satisfies a linear differential equation (28) and has the zero initial condition, $F(y_0, \sigma)$ must be zero for all σ, thus $F(y_0, \sigma) = 0$. According to the definition (27), this is equivalent to (6).

Equation (7) can be proved in an analogous way. Consider the function

$$G(y_0, \sigma) = \frac{\partial u}{\partial \sigma} - \nabla_0 u \cdot R(y_0) - r(y_0) = r(y) - r(y_0) - \nabla_0 u \cdot R(y_0)\ . \tag{29}$$

At $\sigma = 0$, $G(y_0, 0)$ is zero due to the zero initial conditions on u.

Additionally, at any σ,

$$\begin{aligned} \frac{\partial G}{\partial \sigma} &= r'(y) \cdot \frac{\partial y}{\partial \sigma} - \nabla_0 \frac{\partial u}{\partial \sigma} \cdot R(y_0) \\ &= r'(y) \cdot R(y) - \nabla_0 r(y) \cdot R(y_0) \\ &= r'(y) \cdot [R(y) - \nabla_0 y\, R(y_0)] \\ &= r'(y) \cdot F(y_0, \sigma) = 0\ , \end{aligned}$$

Hence, $G(y_0, \sigma)$ is identically equal to zero, which is equivalent to equation (7).

Finally, we point out that solutions of the Liouville equations are transported along the same characteristics as solutions of the Hamilton Eqn. 1, only with the trajectory parameter running backward. This reflects the reciprocity of the Hamiltonian system: initial conditions are restored by backward ray tracing.

Acknowledgements: We thank A. Chorin, O. Hald, and M. Popovici for many valuable discussions concerning Liouville equations and multiple arrivals.

References

[1] Audebert, F., Nichols, D., Rekdal, T., Biondi, B., Lumley, D. E. and Urdaneta, H., 1997, Imaging complex geologic structure with single-arrival Kirchhoff prestack depth migration: Geophysics, 62, 1533-1543.

[2] Benamou, J.D., *Big ray tracing : multivalued travel time field computation using viscosity solutions of the eikonal equation*, J. Comp. Physics, 128, 463-474, 1996

[3] Proceedings of the WORKSHOP on the COMPUTATION OF MULTI-VALUED TRAVELTIMES, Ed. Benamou, J-D., INRIA, Sept. 16-18 1996.

[4] Bernasconi, G. and Drufuca, G., *3-D traveltimes and amplitudes by gridded rays*, Geophysics, 66, 277-282, 2001.

[3] O. Hald developed this derivation of the Liouville equation, and we follow it closely.

[5] Cerveny, V. Seismic Ray Theory, Cambridge University Press, 2001.

[6] Chorin, A.,J., Hald, O., Kuperfman, R., *Optimal prediction and the Mori-Zwanzig representation of irreversible processes*, Proc. Nat. Acade., Sciences, USA, 97, pp. 2968-2973, 2000.

[7] Chorin, A.,J., Hald, O., Kuperfman, R., *Non-Markovian optimal prediction*, Monte-Carlo Meth. & Appl.,7, pp. 99-109, 2001.

[8] Crandall, M.G. & Lions, P-L., *Viscosity Solutions of Hamilton-Jacobi Equations*, Tran. AMS, 277, pp. 1-43, 1983.

[9] Crandall, M.G., Evans, L.C. & Lions, P-L., *Some Properties of Viscosity Solutions of Hamilton-Jacobi Equations*, Tran. AMS, 282, pp. 487-502, 1984.

[10] Dijkstra, E.W., *A Note on Two Problems in Connection with Graphs*, Numerische Mathematik, 1, pp. 269-271, 1959.

[11] Duistermaat, J.,J., (1974), Oscillatory integrals, Lagrange immersions and unfolding of singularities, Commum. Pure Appl.Maths., Vol.27, 207-281.

[12] Engquist, B., Runborg, O., and Tornberg, A-K., *The Segment Projection Method for Geometrical Optics*, work in progress, 2001.

[13] Evans, L.C., Partial Differential Equations, American Mathematical Society, 1998.

[14] Fomel, S., and Sethian, J.A., *Multiple Arrivals using Liouville Equations*, LBL Technical Report #48682, April, 2001.

[15] Fomel, S., and Sethian, J.A., *Escape Equations for Computing Multi-Valued Solutions to Static Hamilton-Jacobi Equations*, to be submitted for publication, Sept. 2001.

[16] Geoltrain, S. and Brac, J., 1993, Can we image complex structures with first-arrival traveltime?: Geophysics, 58, 564-575.

[17] Goldin, S. V., *Seismic traveltime inversion*, Soc. Expl. Geophys., Tulsa., 1986.

[18] Gritsenko, S. A., 1984, *Time field derivatives*: Soviet Geology and Geophysics, 25, no. 4, 103-109, 1984.

[19] Plimpton, S., Hendrickson, B., Burns, S., and McLendon, W. *Parallel Algorithms for Radiation Transport on Unstructured Grids*, Proceedings from Supercomputing '00, 2001.

[20] Klimes, L., *Grid travel-time tracing: Second-order method for the first arrivals in smooth media*, PAGEOPH, 148, 539-563, 1996.

[21] Lambare, G., Lucio, P.S. and Hanyga A., *Two-dimensional multivalued traveltime and amplitude maps by uniform sampling of a ray field*, Geophys. J. Int., 125, 584-598, 1996..

[22] Lasaint, P., and Raviart, P.A., *Finite Element Methods and the Neutron Transport Equation*, in Mathematical Aspects of Finite Element Partial Differential Equations, Ed. De Boor, C., Academic Press, London, 1974.

[23] Maslov, V.P., and Fedoriuk, M.V., (1981), Semi-classical approximations in quantum mechanics, Reidel, Dordrecht.

[24] Ruuth, S., Merriman, B., and Osher, S., *A Fixed Grid Method for Capturing the Motion of Self-Intersecting Wavefronts and Related PDEs*, J. Comp. Phys., 163, 1, pp. 1-21, 2000.

[25] Sanz-Serna, J.M. and Calvo, M.P. Numerical Hamiltonian Problems, CRC Press, 1994.

[26] Sava, P. and Fomel, S., *3-D traveltime computation using Huygens wavefront tracing*, Geophysics, 66, 883-889, 2001.

[27] Sethian, J.A., *A Fast Marching Level Set Method for Monotonically Advancing Fronts*, Proc. Nat. Acad. Sci., 93, 4, pp. 1591-1595, February 1996.

[28] Sethian, J.A. & Popovici, M., *Three Dimensional Traveltimes Computation Using the Fast Marching Method*, Geophysics, 64, 2, 1999.

[29] Sethian, J.A., Level Set Methods and Fast Marching Methods: Evolving Interfaces in Computational Geometry, Fluid Mechanics, Computer Vision and Materials Sciences, Cambridge University Press, 1999.

[30] Sethian, J.A., and Vladimirsky, A., *Ordered Upwind Methods for Static Hamilton-Jacobi Equations*, to appear, Proceedings of the National Academy of Sciences, 2001.

[31] Sethian, J.A., and Vladimirsky, A., *Ordered Upwind Methods for Static Hamilton-Jacobi Equations: Theory and Algorithms*, Center for Pure and Applied Mathematics Technical Report PAM-792, University of California, Berkeley; submitted for publication, SIAM Journal Numerical Analysis, July 2001.

[32] Steinhoff, J., Fan, M., Wang, L., *A New Eulerian Method for the Computation of Propagating Short Acoustic and Electromagnetic Pulses*, J. Comp. Phys., 157, 2, pp. 683-706, 2000.

[33] Symes, W.W., *A slowness matching finite difference algorithm for traveltimes beyond transmission caustics*, Proceedings, 68th Annual International Meeting of the Society of Exploration Geophysicists, New Orleans, Expanded astract, (1998).

[34] Sethian, J.A., *Fast Marching Methods*, SIAM Review, Vol. 41, No. 2, pp. 199-235, 1999.

[35] Xu, S., Chauris, H., Lambare, G. and Noble, M. S., 1998, Common angle image gather: A new strategy for imaging complex media, 68th Ann. Internat. Mtg: Soc. of Expl. Geophys., 1538-1541.

[36] Vinje, V., Iversen, E. and Gjoystdal, H., *Traveltime and amplitude estimation using wavefront construction*, Geophysics, 58, 1157-1166, 1993.

Ernest Orlando Lawrence Berkeley National Laboratory
One Cyclotron Road | Berkeley, California 94720

Prepared for the U.S. Department of Energy under Contract No. DE-AC03-76SF00098